Nanostructures

DOI: 10.1002/anie.200703817

Charge Separation in Layered Titanate Nanostructures: Effect of Ion Exchange Induced Morphology Transformation**

*Alexander Riss, Thomas Berger, Slavica Stankic, Johannes Bernardi, Erich Knözinger, and Oliver Diwald**

Morphology changes induced by surface chemistry can provide important insights into photoexcitation processes on solids which are critical to photovoltaic and photocatalytic applications.[1–3] This area is of particular relevance for TiO_2-based nanomaterials, which have become available as sheets, wires, tubes, and rods only recently.[4–8] We investigated charge-separation processes on $Na_2Ti_3O_7$ nanowires and scrolled-up $H_2Ti_3O_7$ nanotubes, two types of morphologies which can reversibly be transformed into each other by acid/base treatment. A complementarity between efficient charge separation and the radiative recombination of photoexcited states clearly demonstrates that morphology and interlayer composition have a critical influence on the photoelectronic properties of layered oxide nanostructures.

Layered transition-metal oxide structures can be described as stacked polyanion sheets of interconnected $[MO_6]^{n-}$ octahedra with intercalated cations in the interlayer region.[9] While the negatively charged metal oxide sheet exhibits strong intrasheet covalent bonds, those between the sheets are actually relatively weak. For this reason, surface chemistry can induce sheet exfoliation[5,6] upon formation of two-dimensional solids with sometimes unexpected properties, such as strongly enhanced acidity[10] or surface structures that do not exist in corresponding three-dimensional compounds.[11–13] Phenomena that prevail on anisotropic and morphologically well-defined nanostructures have become accessible for exploration thanks to recent advances in materials chemistry.[14–19]

For the production of $Na_2Ti_3O_7$ nanowires like those shown in Figure 1a, we heated commercial TiO_2 (Alfa Aesar no. 36199) in an aqueous solution of 10 N NaOH at reflux (380 K).[6,19,20] With lengths of several hundreds of nanometers, $Na_2Ti_3O_7$ nanowires represent layered and massive structures with diameters between 10 and 100 nm. Corresponding Raman spectra show only bands that are consistent with those reported for titanate nanostructures.[19,21] High-resolution transmission electron micrographs reveal relatively smooth surfaces and parallel-oriented lattice fringes with interlayer spacings of 7.5 ± 0.7 Å (Figure S1b in the Supporting Information).[19]

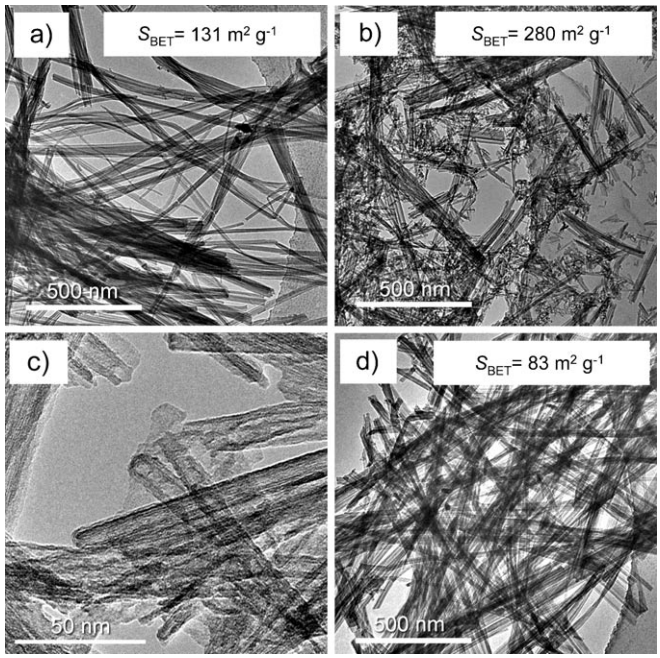

Figure 1. Low-magnification TEM images of $Na_2Ti_3O_7$ nanowires (a) generated by treatment of TiO_2 powders in aqueous NaOH solution ($S_{BET} = 131\ m^2\,g^{-1}$). Washing these nanowires with 0.1 N HCl transforms them into much smaller $H_2Ti_3O_7$ nanotubes (b and c), which gives rise to significantly enhanced specific surface areas ($S_{BET} = 280\ m^2\,g^{-1}$). After contact with 10 N NaOH, $H_2Ti_3O_7$ nanotubes disappear upon regeneration of massive titanate nanowires (d), a process which is accompanied by a significant decrease of specific surface area to 83 $m^2\,g^{-1}$.

Inconsistent with other reports,[22,23] acidic treatment of nanowires was essential in our work for their transformation into tubes. Washing $Na_2Ti_3O_7$ nanowires with 0.1 N HCl causes replacement of the sodium ions by protons and, at the same time, produces much smaller structures than nanowires (for comparison, Figure 1b characterizes a sample in which both qualities are present). Figure 1c shows a typical high-resolution image of scrolled and multiwalled $H_2Ti_3O_7$ nanotubes with approximately 4 and 12 nm as inner and outer diameters, respectively. As a major result of this study, we found that the

[*] A. Riss, T. Berger, S. Stankic, E. Knözinger, O. Diwald
Institute of Materials Chemistry
Vienna University of Technology
Veterinärplatz 1/GA, 1210 Vienna (Austria)
Fax: (+43) 1-25077-3890
E-mail: odiwald@mail.zserv.tuwien.ac.at
Homepage: http://www.imc.tuwien.ac.at
J. Bernardi
University Service Centre for Transmission Electron Microscopy
Vienna University of Technology
Wiedner Hauptstrasse 8–10/137, 1040 Vienna (Austria)

[**] This work was financially supported by the Austrian Fonds zur Förderung der Wissenschaftlichen Forschung (FWF—P17514-N11), which is gratefully acknowledged. We thank Hinrich Grothe for his assistance with the Raman measurements and Nicolas Siedl for his comments on this manuscript.

Supporting information for this article is available on the WWW under http://www.angewandte.org or from the author.

room-temperature conversion of larger-sized wires for which the corresponding powder exhibits a specific surface area of $S_{BET} = 131\ m^2 g^{-1}$ into highly dispersed $H_2Ti_3O_7$ nanotubes with $S_{BET} = 280\ m^2 g^{-1}$ can be reversed.[24] Suspension of nanotubes in 10 N NaOH solution generates nanowires (Figure 1 d, and Figure S2 in the Supporting Information) which—in terms of structure and morphology—are identical to those characterized in Figure 1 a. With TEM, we also observed unscrolled nanosheet remnants as well as details of the attachment of exfoliated sheets to larger nanowire fragments (Figure S2 in the Supporting Information). It is important to note that for both types of morphologies investigated, wires and tubes, the Raman spectra revealed bands that are consistent with layered $Na_xH_{2-x}Ti_3O_7$ titanate structures (Figure S3 in the Supporting Information).[21,25]

The surface chemistry induced transformation of larger-sized titanate wires into nanotubes and its reversal[6,26] are explained by means of Figure 2. Acid treatment of titanate wires induces delamination into sheets, which then scroll up and form multiwalled nanotubes. The delamination process is driven by the concentration gradient of H^+ or Na^+ ions perpendicular to the outermost titanate layer.[6,27] The limiting radius of the titanate nanotubes and thus the morphological uniformity observed are ascribed to the balance between the difference in surface energy and the lattice strain induced by bending.[4,6,27] Theoretical calculations have predicted the protonation-induced distortion of the TiO_6 units from octahedral geometry.[27] This effect is reversed when protons are replaced by more weakly bonded Na^+ ions. As a consequence of such a change, nanotubes unscroll into flat nanosheets, which can laterally attach to each other, form multilayered stacks, and finally produce massive titanate nanowires (Figure 1 d, and Figure S2 of the Supporting Information).

Despite a variety of reports on the photoactivity of layered TiO_2-based nanostructures suspended in the liquid phase,[6,28,29] we are not aware of any corresponding study that concentrates on the gas–solid interface. Prior to UV excitation studies of the wires and tubes, we applied vacuum annealing at 470 K and $p < 10^{-5}$ mbar to remove physisorbed water from these high-surface-area materials. TEM measurements showed that such activation steps did not change their structure and morphology. To investigate the transfer of photogenerated charges across the gas–solid interface of titanate nanowires and tubes, we employed O_2 as an electron scavenger. Specifically, with the use of EPR spectroscopy, surface O_2^- radicals have successfully been used to probe specific sites on TiO_2 particle surfaces,[30–32] to quantify the number of trapped charges,[33] or to monitor photochemical reactivity of doped TiO_2 structures in the range of visible light.[34] Critical to photocatalysis, scavenging of photogenerated electrons by O_2 allows for the accumulation of reactive hole centers and enhances the efficiency of the overall reaction.[33,35,36]

Typical EPR spectra measured on titanate wires and tubes after photoexcitation at 140 K and normalized to the same surface area are plotted in Figure 3 a. Only a negligible concentration of paramagnetic products originates from photoexcitation of the nanowires. However, in the case of titanate nanotubes (Figure 1 b,c) the concentration of paramagnetic sites is significantly enhanced. EPR signal analysis by spectrum simulation points to the presence of essentially two paramagnetic centers: 1) O_2^- radicals which are characterized by the g-tensor components $g_1 = 2.0198$, $g_2 = 2.0093$, and $g_3 = 2.0033$ and result from efficient transfer of photogenerated electrons from the solid to adsorbed O_2; 2) a paramagnetic defect at $g = 2.0031$ that—to 70 % of the intensity plotted in Figure 3 a—is already detectable on vacuum-annealed titanate tubes, an observation also made by others.[37,38] At present, the exact nature of the underlying defect remains open and is subject to ongoing work. In contrast to completely dehydroxylated TiO_2 nanocrystals,[33] we do not observe paramagnetic hole centers in the form of O^- radicals on protonated titanate nanotubes after UV excitation. This result is attributed to constitutional OH

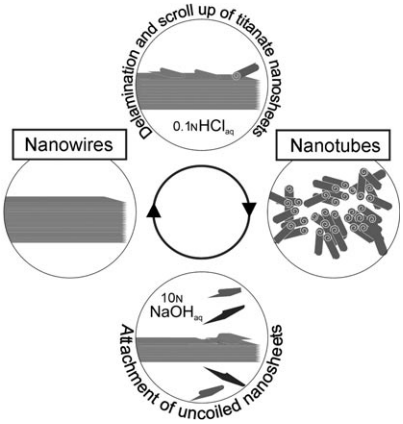

Figure 2. Reversible acid/base-induced interconversion of $Na_2Ti_3O_7$ nanowires into $H_2Ti_3O_7$ nanotubes.

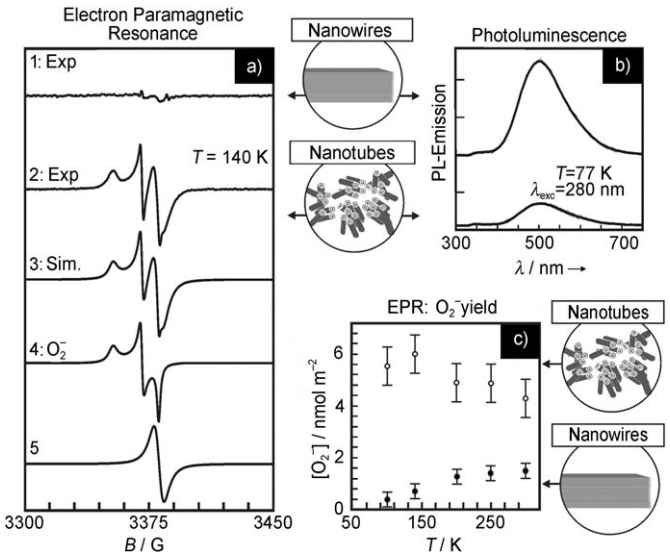

Figure 3. a) EPR and b) photoluminescence spectra of photoexcited titanate nanowires and -tubes (curves 1 and 2, respectively). In part (a), the simulated spectrum of the titanate nanotubes is shown as curve 3, which is divided into its two component spectra: that of O_2^- (curve 4) and an unknown paramagnetic defect (curve 5). For charge-carrier trapping, UV excitation with 10^{15} photons $cm^{-2} s^{-1}$ was carried out in the presence of 7 mbar O_2 for $t_{UV} = 2400$ s (a). c) After subsequent evacuation to 10^{-6} mbar, surface-adsorbed oxygen radicals were measured at various temperatures.

groups present at the interfaces of the curved titanate nanosheets. We expect that these hydroxyl groups mediate the transformation of trapped holes into diamagnetic product states via short-lived OH radicals as intermediates.[39,40]

Complementing the EPR measurements, we also characterized the photoluminescence properties of the $Na_2Ti_3O_7$ nanowires and $H_2Ti_3O_7$ nanotubes (Figure 3b). Induced by $\lambda = 282$ nm excitation light, an emission band at $\lambda = 505$ nm was observed on titanate nanowires at 77 K and attributed to trapped exciton states.[19] This phenomenon is only observable below 298 K owing to thermal quenching effects. As another important characteristic, the respective photoemission process is strongly suppressed in titanate nanotubes (Figure 3b).[19] Retransformation of the nanotubes into wires restores the photoluminescence properties and reduces the concentration of paramagnetic sites to the same level as in the starting material.

Searching for a correspondence between photoluminescence[41] and the solids' capability for persistent charge separation, we measured the yield of scavenged electrons in the range between 100 and 300 K and plotted the O_2^- radical concentration per unit surface area in Figure 3c.[33] Over the entire temperature range, charge separation occurs on tubes with much higher efficiencies than on wires. After photoexcitation of the nanotubes at 140 K the O_2^- concentration amounts to $(6 \pm 2) \times 10^{-9}$ mol m^{-2}, which, assuming an average length of 100 nm and the nanotube dimensions mentioned above, corresponds to 30 ± 10 radicals per nanotube.

Differences in temperature dependence of the charge-separation yield indicate that there is no simple anticorrelation between the photoluminescence emission intensity and the extent of charge separation. Additional factors such as changed adsorption properties must play a role.[33] Even so, chemical changes in the interlayer region are expected to alter the potential-energy surface in such a way that the exciton does not localize within the TiO_6 unit anymore.[19] Consequently, we expect an increase in the lifetime of the photoexcited state, which then becomes susceptible to decomposition into electrons and holes.

Furthermore, titanate nanotubes represent curved structures such that the underlying self-organization process is determined by the balance between surface-energy minimization and lattice strain induced by bending.[6,27] In insulating solids elastic-strain gradients can generate electric polarization of the lattice,[42] which likely favors charge separation and, thus, interfacial electron transfer to surface-adsorbed O_2. Related observations were made on barium titanates, where those with tunnel structure exhibit enhanced photocatalytic activity.[43] Certainly, further studies on these multifunctional materials are required to understand the detailed physics which control the branching ratio between formation and radiative deactivation of photoexcited states and their decomposition.

Radiative and nonradiative recombination of charge carriers compete with the chemical utilization of photogenerated charges at the surface.[44] To optimize the desired functionality of TiO_2-based devices,[1,2,6] the branching ratio between these key processes has to be controlled. The fact that ion exchange and morphology transformation can easily be accomplished by soft chemical treatment provides efficient means for controlling the photoelectronic properties of uniformly sized and morphologically well-defined nanostructures. This is of great importance for their use as a medium for electron- and/or energy-transfer processes, for the improvement of their photocatalytic activities, and for the achievement of higher photovoltaic efficiencies.

Finally, we note that the reversible interconversion of titanate nanowires with plane surfaces and interfaces into curved tubes with local strain effects gives another example for the great potential of morphologically well-defined nanomaterials as model systems. The enhancement or depletion of the abundance of different morphological characteristics (such as nanocube corners,[45] specific surface planes,[18] or tips of high-aspect-ratio nanoparticles[6]) can be utilized to obtain valuable insights into physical and chemical surface functionalities.[46]

In summary, we report on the effect of surface chemistry induced morphology transformation on the charge-separation properties of layered oxide materials. There is a clear complementarity between titanate morphologies that are associated with photoluminescence in conjunction with inhibited charge separation and those with the opposite properties. The respective trends and, thus, the branching ratio between radiative deactivation and chemical utilization of photoexcited states can easily be controlled by solution chemistry. These findings are of great importance for new concepts in the synthesis of photoactive materials as well as for the use of related nanostructures as model systems for in-depth physical and chemical studies. Owing to the variety of related applications that are based on gas–solid interface effects,[1,47,48] there is a growing need for surface-science investigations on layered oxides of various morphologies[13,49]

Experimental Section

In a typical synthetic procedure, commercial anatase powder (5 g, Alfa Aesar no. 36199) was treated with 10 N NaOH (300 mL) at 380 K under reflux for 48 h. The obtained product is denoted as $Na_2Ti_3O_7$ titanate nanowires. A part of the sample was treated with 0.1 N HCl four times to give $H_2Ti_3O_7$ titanate nanotubes. Both samples were washed with distilled water and dried at room temperature. Thermal activation at 473 K and $p < 10^{-5}$ mbar represented the final step of sample preparation.

TEM images were obtained using a TECNAI F20 analytical microscope equipped with an S-Twin objective lens and a field emission source operating at 200 kV. Images were recorded with a Gatan 794 Multiscan CCD camera.

For EPR measurements approximately 20 mg of the powder sample was contained within a Suprasil quartz glass tube which was connected to an appropriate high-vacuum pumping system providing base pressures better than $p = 10^{-6}$ mbar. A 300 W Xe lamp (Oriel) was employed as the UV source. The light beam was passed through a water filter to exclude IR contributions from the excitation spectrum. Light power was measured with a bolometer (International Light) and kept constant at 0.7 mW cm^{-2} for the wavelength range 200–380 nm throughout all experiments. X-band EPR measurements were performed with a Bruker EMX 10/12 spectrometer using an ER 4102 ST standard rectangular resonant cavity in the TE102 mode. Low-temperature measurements were carried out with an ER 4131 VT variable-temperature accessory which operates in the temperature range between 90 and 300 K. The g values were determined on the basis of a diphenylpyricylhydrazil (DPPH) standard.

A pulsed Xe discharge lamp served as the excitation light source in a Perkin-Elmer LS 50B system for photoluminescence measurements. Measurements were carried out at 77 K using a commercially available low-temperature luminescence accessory in which the sample cell was held by a high-purity copper rod that was immersed in liquid nitrogen. For both types of spectroscopic measurements the identical sample volumes with comparable powder densities were exposed to UV light.

The nitrogen sorption isotherms were obtained at 77 K using an adsorption porosimeter (Micromeritics ASAP 2020). The BET surface area (S_{BET}) was evaluated using adsorption data in a relative pressure range p/p_0 from 0.05 to 0.2. The absence of a prominent feature at 2–6 nm in the pore size distribution indicates that the internal volume of the tubes is not accessible to small molecules like N_2 or O_2.

Received: August 20, 2007
Revised: October 8, 2007
Published online: January 10, 2008

Keywords: charge trapping · EPR spectroscopy · luminescence · nanostructures · photochemistry

[1] T. L. Thompson, J. T. Yates, *Chem. Rev.* **2006**, *106*, 4428 – 4453.
[2] P. V. Kamat, *J. Phys. Chem. C* **2007**, *111*, 2834 – 2860.
[3] J. M. Macak, M. Zlamal, J. Krysa, P. Schmuki, *Small* **2007**, *3*, 300 – 304.
[4] a) G. R. Patzke, F. Krumeich, R. Nesper, *Angew. Chem.* **2002**, *114*, 2554 – 2571; *Angew. Chem. Int. Ed.* **2002**, *41*, 2446 – 2461.
[5] Y. B. Mao, S. S. Wong, *J. Am. Chem. Soc.* **2006**, *128*, 8217 – 8226.
[6] Z. V. Saponjic, N. M. Dimitrijevic, D. M. Tiede, A. J. Goshe, X. Zuo, L. X. Chen, A. S. Barnard, P. Zapol, L. Curtiss, T. Rajh, *Adv. Mater.* **2005**, *17*, 965 – 971.
[7] Y. Mao, T. J. Park, F. Zhang, H. Zhou, S. S. Wong, *Small* **2007**, *3*, 1122 – 1139.
[8] D. V. Bavykin, J. M. Friedrich, F. C. Walsh, *Adv. Mater.* **2006**, *18*, 2807 – 2824.
[9] R. E. Schaak, T. E. Mallouk, *Chem. Mater.* **2002**, *14*, 1455 – 1471.
[10] A. Takagaki, M. Sugisawa, D. Lu, J. N. Kondo, M. Hara, K. Domen, S. Hayashi, *J. Am. Chem. Soc.* **2003**, *125*, 5479 – 5485.
[11] K. Zhu, J. Hu, C. Kübel, R. Richards, *Angew. Chem.* **2006**, *118*, 7435 – 7439; *Angew. Chem. Int. Ed.* **2006**, *45*, 7277 – 7281.
[12] J. Goniakowski, C. Noguera, L. Giordano, *Phys. Rev. Lett.* **2007**, *98*, 205701.
[13] T. Orzali, M. Casarin, G. Granozzi, M. Sambi, A. Vittadini, *Phys. Rev. Lett.* **2006**, *97*, 156101.
[14] G. A. Ozin, A. C. Arsenault in *Nanochemistry, A Chemical Approach to Nanomaterials*, RSC publishing, Cambridge, UK, **2006**.
[15] A. Testino, I. R. Bellobono, V. Buscaglia, C. Carnevali, M. D'Arienzo, S. Polizzi, R. Scotti, F. Morazzoni, *J. Am. Chem. Soc.* **2007**, *129*, 3564 – 3575.
[16] C. Burda, X. B. Chen, R. Narayanan, M. A. El-Sayed, *Chem. Rev.* **2005**, *105*, 1025 – 1102.
[17] V. I. Klimov, *J. Phys. Chem. B* **2006**, *110*, 16827 – 16845.
[18] S. C. Erwin, L. Zu, M. I. Haftel, A. L. Efros, T. A. Kennedy, D. J. Norris, *Nature* **2005**, *436*, 91.
[19] A. Riss, T. Berger, H. Grothe, J. Bernardi, O. Diwald, E. Knözinger, *Nano Lett.* **2007**, *7*, 433 – 438.
[20] A. R. Armstrong, G. Armstrong, J. Canales, P. G. Bruce, *Angew. Chem.* **2004**, *116*, 2336 – 2338; *Angew. Chem. Int. Ed.* **2004**, *43*, 2286 – 2288.
[21] R. Ma, K. Fukuda, T. Sasaki, M. Osada, Y. Bando, *J. Phys. Chem. B* **2005**, *109*, 6210 – 6214.
[22] C.-C. Tsai, H. Teng, *Chem. Mater.* **2006**, *18*, 367 – 373.
[23] Q. Chen, W. Z. Zhou, G. H. Du, L. M. Peng, *Adv. Mater.* **2002**, *14*, 1208 – 1211.
[24] The material shown in Figure 1b was obtained after four iterations of HCl treatment whereby less than 100% of the nanowires were transformed into tubes. This result explains why the specific surface area of 280 $m^2 g^{-1}$ is less than a value one would expect on the basis of geometrical considerations.
[25] X-ray diffraction measurements did not reveal unambiguous structural information since broadened reflections in the XRD pattern resulting from limited coherence area made interpretations and their assignment very difficult.
[26] A. Banard, Z. Saponjic, D. Tiede, L. Curtiss, *Rev. Adv. Mater. Sci.* **2005**, *10*, 21 – 27
[27] S. Zhang, Q. Chen, L.-M. Peng, *Phys. Rev. B* **2005**, *71*, 014104.
[28] T. Tachikawa, S. Tojo, M. Fujitsuka, T. Sekino, T. Majima, *J. Phys. Chem. B* **2006**, *110*, 14055 – 14059.
[29] H. Y. Song, H. F. Jiang, T. Liu, X. Q. Liu, G. Y. Meng, *Mater. Res. Bull.* **2007**, *42*, 334 – 344.
[30] M. Che, A. J. Tench, *Adv. Catal.* **1983**, *32*, 1 – 148.
[31] M. Anpo, M. Che, B. Fubini, E. Garrone, E. Giamello, M. C. Paganini, *Top. Catal.* **1999**, *8*, 189 – 198.
[32] E. Carter, A. F. Carley, D. M. Murphy, *J. Phys. Chem. C* **2007**, *111*, 10630 – 10638.
[33] T. Berger, M. Sterrer, O. Diwald, E. Knözinger, *ChemPhysChem* **2005**, *6*, 2104 – 2112.
[34] S. Livraghi, M. C. Paganini, E. Giamello, A. Selloni, C. Di Valentin, G. Pacchioni, *J. Am. Chem. Soc.* **2006**, *128*, 15666 – 15671.
[35] C. Wang, A. Heller, H. Gerischer, *J. Am. Chem. Soc.* **1992**, *114*, 5230 – 5234.
[36] M. A. Henderson, J. M. White, H. Uetsuka, H. Onishi, *J. Catal.* **2006**, *238*, 153 – 164.
[37] S. L. Zhang, W. Li, Z. S. Jin, J. J. Yang, J. W. Zhang, Z. L. Du, Z. J. Zhang, *J. Solid State Chem.* **2004**, *177*, 1365 – 1371.
[38] The EPR properties of this center are consistent with those of electron centers identified in aggregated TiO_2 nanocrystals (see [M. J. Elser, T. Berger, D. Brandhuber, J. Bernardi, O. Diwald, E. Knözinger, *J. Phys. Chem. B* **2006**, *110*, 7605 – 7608). We expect that the associated defect is located underneath the surface since only limited interaction with paramagnetic O_2 from the gas phase was observed.
[39] O. I. Micic, Y. N. Zhang, K. R. Cromack, A. D. Trifunac, M. C. Thurnauer, *J. Phys. Chem. B* **1993**, *97*, 7277 – 7283.
[40] Y. Murakami, K. Endo, I. Ohta, A. Y. Nosaka, Y. Nosaka, *J. Phys. Chem. C* **2007**, *111*, 11339 – 11346.
[41] In contrast to nanoparticles stabilized in optically transparent suspensions, we cannot specify the quantum yield of photoluminescence processes measured on powders, since scattering effects render the quantification of particles reached by excitation light and those detected by photoluminescence emission impossible.
[42] L. E. Gross, *J. Mater. Sci.* **2006**, *41*, 53 – 63.
[43] a) M. Kohno, K. Sato, Y. Inoue, *Phys. Chem. Chem. Phys.* **1999**, *1*, 179 – 183; b) M. Kohno, S. Ogura, K. Sato, Y. Inoue, *Stud. Surf. Sci. Catal. A&B* **1996**, *101*, 143 – 152.
[44] T. Berger, M. Sterrer, O. Diwald, E. Knözinger, J. T. Yates, Jr., *Phys. Chem. Chem. Phys.* **2006**, *8*, 1822 – 1826.
[45] S. Stankic, M. Müller, O. Diwald, M. Sterrer, E. Knözinger, J. Bernardi, *Angew. Chem.* **2005**, *117*, 4996 – 4999; *Angew. Chem. Int. Ed.* **2005**, *44*, 4917 – 4920.
[46] a) H. Lee, S. E. Habas, S. Kweskin, D. Butcher, G. A. Somorjai, P. Yang, *Angew. Chem.* **2006**, *118*, 7988 – 7992; *Angew. Chem. Int. Ed.* **2006**, *45*, 7824 – 7828.
[47] U. Diebold, *Surf. Sci. Rep.* **2003**, *48*, 53 – 229.
[48] A. Gurlo, R. Riedel, *Angew. Chem.* **2007**, *119*, 3900 – 3923; *Angew. Chem. Int. Ed.* **2007**, *46*, 3826 – 3848.
[49] S. Funk, B. Hokkanen, U. Burghaus, A. Ghicov, P. Schmuki, *Nano Lett.* **2007**, *7*, 1091 – 1094.

